Desalination and Water Treatment
www.deswater.com

doi: 10.5004/dwt.2017.0350

62 (2017) 221–234
February

Mechanisms of para-chlorophenol adsorption onto activated carbons having different textural and chemical properties

Etelka Dávid[a], Marius Sebastian Secula[a], Günseli Özdemir[b,*], Ioan Mămăligă[a,*]

[a]*Department of Chemical Engineering, Faculty of Chemical Engineering and Environmental Protection, TUIASI – Gheorghe Asachi Technical University of Iasi, 73, Prof. Dr. Doc. D. Mangeron, 700050, Iasi, Romania, Tel. +40232-278683; Fax: +40232- 271311; emails: etelkadavid@yahoo.com (E. David), mariussecula@yahoo.com (M.S. Secula), imamalig@tuiasi.ro (I. Mamaliga)*
[b]*Department of Chemical Engineering, Faculty of Engineering, Ege University, Bornova, 35100 Izmir, Turkey, email: gunseli.ozdemir@ege.edu.tr*

Received 27 March 2016; Accepted 8 July 2016

ABSTRACT

The present study describes the adsorption behavior, mechanisms governing the process and thermodynamics of the separation of *p*-chlorophenol (4-CP) from aqueous solutions by several granular activated carbons (ACs). The main contribution of this work consists in bringing more insight onto the proper selection of sorbents based on the affinity between them and a specific sorbate with a special regard onto the textural and chemical characteristics of sorbents. Batch tests were conducted in order to evaluate the kinetics, equilibrium and thermodynamics of each considered adsorption system. Equilibrium data were fitted to Langmuir, Freundlich, Sips, Redlich–Peterson and Radke–Prausnitz isotherms in order to elucidate the mechanisms governing the adsorption processes. Also, the kinetics data were analyzed by means of pseudo-first-order, pseudo-second-order, and intraparticle diffusion models The best-fitted adsorption isotherm models were found to be in the order Sips > Redlich–Peterson > Freundlich > Radke–Prausnitz > Langmuir, and the pseudo-second-order model described best the behavior of the adsorption of 4-CP onto each of the five investigated ACs. The adsorption capacity of the AC was found to decrease with temperature. The process of 4-CP adsorption onto AC was spontaneous, and physical in nature and thermodynamically feasible.

Keywords: Para-chlorophenol; Adsorption; Surface properties; Diffusion; Activated carbon

1. Introduction

Chlorinated phenols are among the most common organic pollutants of wastewaters that require careful treatment before being discharged into the receiving body of waters. The main pollution sources containing monochlorinated phenols are the wastewaters generated by pesticide, paint, solvent, pharmaceuticals, wood preserving chemicals, and paper and pulp industries. When chlorination is used to disinfect water, chlorinated phenols are generated [1]. Chlorophenols are of major concern in view of their widespread contamination of soil and potable groundwater supplies and their harmful effects on humans and animals. Having low biological degradability, high toxicity, and high ecological endurance, they pose serious problems and therefore extensive research work has been made in recent years in order to minimize phenol concentration in wastewaters [2–6]. The US Environmental Protection Agency (EPA) regulations call for lowering phenol content in wastewater to less than 1 ppm [7]. Also, EPA has listed phenolic compounds as precedence compounds [8]. The guideline proposed by the World Health Organization (WHO) for phenol concentration in drinking water is < 2 μg L^{-1} [9]. It has been reported that 0.01 mg L^{-1} of chlorophenols imparts extremely disagreeable taste and odor to water. *p*-Chlorophenol in particularly has low taste and odor thresholds and reference levels of 10 μg L^{-1} proposed as maximum allowed concentration for abstraction

* Corresponding author.

to potable water supply [10]. Among the monochlorinated simple phenols *p*-chlorophenol (C_6H_5ClO, 4-CP) seems to have the highest toxicity level, and it is classified as a hazardous substance due to the fact that it may cause long-term adverse effects in the aquatic environment [11]. Also, Deka and Bhattacharyya [12] pointed out that chlorine at the *para* position is the most difficult to remove. *Para*-chlorophenol is used as model pollutant due to its valuable particularities such as: toxicity even at low concentrations, formation of substituted compounds during disinfection and oxidation processes, phytotoxicity and ability to bioaccumulate in organisms, that have similarities with persistent organic pollutants [13,14].

Berestovskaya et al. [15] showed that 4-CP is generated through the degradation of 2,4-dichlorophenoxyacetic acid by anaerobic biological treatment and is further released as micropollutant in aqueous environment [16].

Biological treatment, activated carbon (AC) adsorption, reverse osmosis, ion exchange, and solvent extraction are the most widely used methods for removing phenol and its derivatives from wastewaters. Adsorption is an effective and widely used method to remove phenols from wastewater due to its higher capability and its relatively simple operability [17,18]. Despite many research studies on new adsorbent materials, AC is among the most popular adsorbents, used technically due to its high adsorption capacity, high-surface-area, pore volume, and porosity, coupled with cost effectiveness. It is usually derived from natural materials (e.g., coal, wood, straw, fruit stones, and shells) and manufactured to precise surface properties. A typical AC particle has a porous structure consisting of a network of interconnected macropores, mesopores, and/or micropores that provide a good capacity for the adsorption of organic molecules [19].

There are two most common physical forms in which AC is used, i.e., powder-like and granular AC. In liquid-phase adsorption, the adsorption capacity of AC for aromatic compounds, whether in a powdered or granular form, depends on a number of factors [20]: (i) the physical nature of the adsorbent—pore structure, ash content, functional groups; (ii) the nature of the adsorbate, its p*Ka* value, functional groups, polarity, molecular weight, size; and (iii) the solution conditions such as pH, ionic strength, and the adsorbate concentration. Different raw materials and manufacturing processes produce final AC products with different adsorption characteristics.

While carbon-based adsorption systems have been widely used [21–23], there is still a need for fundamental data such as uptake kinetics and equilibrium parameters particularly in the case of chlorophenols in order to facilitate the design of an adsorption process. The adsorption affinity of phenolic compounds to ACs and other type of adsorbents depends on a multitude of interactions. These interactions take place between the heterogeneously introduced functional groups (such as hydrophobic effect between the aromatic phenolic ring and the graphitic structures, electron donor-acceptor interactions with the basic surface, oxygen and nitrogen) and/or the aromatic surface groups, and the π-π stacking of aromatic phenolic ring [16,17,24–26]. Therefore, this study aims to clarify the effect of AC type on the adsorbability of 4-CP. For this purpose, five ACs having different characteristics were used. The main objective of this study is to investigate the effects of initial 4-CP concentration, contact time, temperature and solution pH in relation with the surface characteristics/adsorbent type of AC on the adsorption process. Equilibrium isotherm data were fitted to Langmuir, Freundlich, Sips, Radke–Prausnitz and Redlich–Peterson equations and constants of isotherm equations were determined. Adsorption kinetics of 4-CP onto AC were also analyzed by using pseudo-first order, pseudo-second order and Weber–Morris models to elucidate the adsorption mechanism. Finally, thermodynamic parameters were evaluated using the adsorption data.

2. Materials and methods

2.1. Adsorbents and solute

Five commercial ACs (L27, F22, S21 and X17 supplied by CECA, Arkema Group, France, and C1 purchased from Seachem, USA) were used in this study. AC porosity was determined by means of conventional nitrogen adsorption isotherm at 77 K using a Micromeritics ASAP 2020. The samples were previously degassed at 643 K for 24 h under a residual vacuum of less than 10^{-4} Pa. The adsorption isotherms were analyzed according to the Dubinin theory. The specific microporous volume W_0 ($cm^3\ g^{-1}$) and mean pore size L_0 (nm) were determined based on the linear part of the Dubinin–Radushkevich plot [27]. The external specific surface S_{ext} ($m^2\ g^{-1}$) was calculated from Sing [28] α_S plots. The specific micropore surface S_{micro} ($m^2\ g^{-1}$) was estimated by assuming slit-shaped micropores based on the following equation:

$$S_{micro} = \frac{2W_0}{L_0} \tag{1}$$

Summing up the external specific surface area and the specific surface area of the micropores resulted in the total surface area (S_{tot} in $m^2\ g^{-1}$).

The chemical properties of the adsorbents were determined as well. The ACs were washed before each analysis. Then, they were dried at 353 K for 12 h. The surface oxygen groups were determined according to the Boehm method [29]. A weight of 0.2 g of AC was added into 25 mL of 0.1 mol L^{-1} aqueous solutions of NaOH, Na_2CO_3, $NaHCO_3$, and HCl, respectively. The GAC/solution mixture was placed in a thermostated multi-agitation apparatus at 25°C under mechanical stirring at 150 rpm for 48 h. The suspension was filtered through a 0.45 μm membrane filter and the excess of base or acid was titrated with 0.1 mol L^{-1} solutions of HCl or NaOH, respectively. The carboxyl, phenol, and lactone groups were quantified. The number of surface basic groups was calculated from the amount of HCl which reacts with the carbon. The method of Rivera-Utrilla and Sanchez-Polo [30] was used to determine the point of zero charge (pH_{PZC}).

The 4-CP (>99.5%, purchased from Sigma-Aldrich) was used to prepare the aqueous solutions for the adsorption study. Table 1 shows the principal characteristics of the sorbate.

2.2. Adsorption procedure

Adsorption experiments were conducted in batch mode in 100 mL stoppered conical flasks. Stock solutions were

Table 1
Characteristics of 4-CP [31]

Molecular weight (g/mole)	128.56
Boiling point (°C)	220
Melting point (°C)	40–45
Density (g/mL, 25°C)	1.306
Vapor pressure (49.8°C)	1 mm Hg
Water solubility (g/100 mL, 20°C)	2.7
Molecular size (Å)	6.47 × 4.17
p*Ka*	9.37
σ (Å^2)	33.31

prepared by dissolving the 4-CP in deionized water. To determine the optimum adsorbent amount, a study was accomplished by varying amounts of AC (0.0125 – 0.1 g) contacted with 50 mL of aqueous solutions having 200 ppm 4-CP.

The conical flasks were shaken on a water bath at 298 ± 1 K and 150 rpm. A shaking time of 48 h was chosen based on the kinetic results to reach equilibrium. At the end of the adsorption process the AC was filtered using Whatman filter paper and the residual solution concentration of 4-CP was analyzed by UV-spectrophotometer (Model UV-1800 Shimadzu) with the optimum wavelength set at 280 nm. Blanks containing no AC were done and the loss was considered. The optimum adsorbent amount was determined as 0.4 g L^{-1}.

The kinetic studies were carried out by adding 0.4 g L^{-1} AC to a fixed volume of solution (50 mL) and following the concentration decay of the 4-CP as a function of time. The initial 4-CP concentration was varied in the 40–200 ppm interval (40, 80, 120, 160 and 200 mg L^{-1}, respectively), and the samples were separated at predetermined time intervals (0.5–48 h). The shape of curve for each sorbent–sorbate system depends on several factors, such as initial concentration of the solution, type of sorbent used, temperature, and pH. The other parameters, shaker speed, and type of vessel were kept constant. The uptake of the adsorbate, q_t (mg g^{-1}) at time t, was calculated by the following equation:

$$q_t = (C_0 - C_t)\frac{V}{m} \tag{2}$$

where C_0 is the initial concentration of the adsorbate (mg L^{-1}) and C_t is the concentration of 4-CP in solution at time t (mg L^{-1}).

In order to study the effect of pH on the removal efficiency, experiments were conducted in the pH range of 2.0 to 12.0 using 0.02 g of AC with 50 mL of 200 ppm aqueous 4-CP solution for 48 h at 298 K. The solution pH was adjusted by the addition of 0.2 M HCl or NaOH before mixing 4-CP with the AC. The natural pH of the solution was about 6.

The specific amount of 4-CP adsorbed was calculated using:

$$q_e = (C_0 - C_e)\frac{V}{m} \tag{3}$$

where q_e is the adsorption capacity (mg g^{-1}) in the adsorbent at equilibrium; C_0 and C_e are the initial and equilibrium concentrations of adsorbate (mg L^{-1}), respectively; V is the volume of the aqueous solution (L) and m is the mass (g) of adsorbent.

The effect of temperature on the adsorption characteristics was investigated by determining the adsorption isotherms at 298, 308, and 318 K. The initial concentration was 200 ppm, the AC dose was 0.4 g L^{-1} and the runs were carried out for 48 h.

The percentage removal of 4-CP was calculated using the following relationship:

$$\%\ \text{Removal} = \frac{100(C_0 - C_e)}{C_0} \tag{4}$$

2.2.1. Kinetic models

The kinetic parameters are helpful to define the efficiency of adsorption, as it describes the rate of solute uptake at the sorbent–solution interface, which gives important informations for designing and modeling the processes [32]. The adsorption process was analyzed using three different kinetic models: the pseudo-first-order, pseudo-second-order, and Weber–Morris intraparticle diffusion model.

2.2.1.1. Pseudo-first-order kinetic model Lagergren and Svenska [33] presented a first-order rate equation to describe the kinetic process of liquid-solid phase adsorption, which is believed to be the earliest model pertaining to the adsorption rate based on the adsorption capacity. It is expressed as follows:

$$\frac{dq_t}{dt} = K_1(q_e - q_t) \tag{5}$$

where q_e and q_t are the sorption capacities at equilibrium and at time t, respectively (mg g^{-1}) and K_1 is the rate constant of pseudo-first-order sorption (L min^{-1}). After integration and applying boundary conditions $t = 0$ to $t = t$ and $q_t = q_t$, Eq. (5) becomes:

$$\log(q_e - q_t) = \log q_e - K_1 t \tag{6}$$

When the values of log $(q_e - q_t)$ are linearly correlated with t, K_1 and q_e can be determined from the slope and intercept of the plot of log $(q_e - q_t)$ vs. t, respectively.

2.2.1.2. Pseudo-second-order kinetic model The adsorption kinetics may also be described by pseudo-second-order equation which is based on the adsorption capacity of solid phase [34]. The equation is expressed as:

$$\frac{dq_t}{dt} = K_2(q_e - q_t)^2 \tag{7}$$

where q_e and q_t are the sorption capacity at equilibrium and at time t, (mg g^{-1}), respectively, and K_2 is the rate constant (g (mg·min)$^{-1}$). The integration of the differential equation yields:

$$\frac{t}{q_t} = \frac{1}{K_2 q_e^2} + \frac{t}{q_e} \tag{8}$$

If the pseudo-second-order kinetics is applicable to the experimental data, the plot of t/q_t vs. t of Eq. (8) should give a linear relationship from which q_e and K_2 can be determined from the slope and intercept of the plot, respectively.

2.2.1.3. Intraparticle diffusion model Since the above two models cannot give definite mechanisms, another simplified model is tested. Intraparticle diffusion model used here refers to the theory proposed by Weber and Morris (1962). They characterized intra-particular diffusion using the relationship between sorption capacity and the square root of time as shown below:

$$q_t = K_{\text{dif}} \cdot t^{0.5} + I \tag{9}$$

where K_{dif} (mg (g $h^{0.5})^{-1}$) is the intraparticle diffusion rate constant and the value of I (mg g^{-1}) indicates the thickness of the boundary layer diffusion, the larger the value, the greater is the boundary effect. The initial rates of intraparticle diffusion can be obtained by linearization of the amount of solute adsorbed per unit mass of adsorbent (q_t) against square root of time ($t^{0.5}$). If the plot of q_t vs. $t^{0.5}$ gives a straight line, then the adsorption process is controlled by intraparticle diffusion only. However, if the data exhibit multi-linear plots, then two or more steps influence the sorption process [35].

2.2.2. Equilibrium isotherms

One of the most appropriate methods in designing and assessing the performance of the sorption system is to investigate the sorption isotherms.

In the present study, the experimental equilibrium data of 4-CP adsorption onto AC were modeled using the best fit of two-parameter isotherm models, namely Langmuir and Freundlich, and three-parameter isotherm models, namely Redlich–Peterson, Radke–Prausnitz and Sips.

The Langmuir model [36] is based on the ideal assumption of a monolayer and uniform adsorption surface with fixed number of definite localized sites that are identical and equivalent, with no lateral interactions between molecules adsorbed on neighboring sites. It can be written as:

$$q_e = \frac{Q_{\max} K_L C_e}{1 + K_L C_e} \tag{10}$$

where $Q_{\max}$ is the maximum adsorption capacity (mg g^{-1}) and K_L is a constant related to the free energy of the adsorption (L mg^{-1}). The essential characteristics of Langmuir isotherm can be expressed by a dimensionless constant called separation factor (or equilibrium parameter), R_L, which is defined as:

$$R_L = \frac{1}{1 + K_L C_0} \tag{11}$$

In this context, lower R_L value reflects that adsorption is more favorable. For instance, the adsorption is considered as irreversible when $R_L = 0$, favorable when $0 < R_L < 1$, linear when $R_L = 1$, and unfavorable when $R_L > 1$ [31].

The Freundlich model is an empirical equation for multilayer adsorption, with non-uniform distribution of adsorption heat, and affinities over the heterogeneous adsorbent surface [37]. It can be written as follows:

$$q_e = K_F C_e^{1/n} \tag{12}$$

where K_F (L mg^{-1}) and n are Freundlich constants related to the adsorption capacity and adsorption intensity, respectively.

At present, Freundlich isotherm is widely applied in heterogeneous systems especially for organic compounds. The linear representation of ln q_e vs. ln C_e gives the values for 1/n and ln K_F. The slope, 1/n, ranges between 0 and 1, which is a measure of adsorption intensity or surface heterogeneity, becoming more heterogeneous as its value gets closer to zero.

The Redlich–Peterson (R–Pe) equation is a combination of Langmuir and Freundlich models. This model has three parameters and incorporates the advantageous significance of the previously presented models. The mechanism of adsorption is a hybrid and does not follow ideal monolayer adsorption. R–Pe model can be mathematically described as follows [38]:

$$q_e = \frac{K_{\text{R–Pe}} C_e}{1 + B(C_e)^{\beta}} \tag{13}$$

where $K_{\text{R–Pe}}$ (L g^{-1}) and B (L mg^{-1}) are R–Pe isotherm constants whereas β is an exponent taking values between 0 and 1. R–Pe model has two limiting cases, when β = 1, the Langmuir equation results, whereas when β = 0, R–Pe equation transforms to Henry's law equation. At high liquid-phase concentrations of the adsorbate, Eq. (13) reduces to the Freundlich equation. The model represents adsorption equilibrium over a wide concentration range, that can be applied either in homogeneous or heterogeneous systems due to its versatility [39].

The correlation of Radke–Prausnitz isotherm has three adjustable parameters: $Q_{\max}$, $K_{\text{R-PR}}$ and $m_{\text{R-PR}}$. At high concentrations, this isotherm becomes the Freundlich isotherm [40,41]. It can be expressed as follows:

$$q_e = \frac{Q_{\max} K_{\text{R–Pr}} C_e}{1 + K_{\text{R–Pr}} (C_e)^{m_{\text{R–Pr}}}} \tag{14}$$

where q_e is the adsorbed amount at equilibrium (mg g^{-1}), $Q_{\max}$ is the Radke–Prausnitz maximum adsorption capacity (mg g^{-1}), C_e is the adsorbate equilibrium concentration (mg L^{-1}), $K_{\text{R–Pr}}$ is the Radke–Prausnitz equilibrium constant (L mg^{-1}), and $m_{\text{R–Pr}}$ is the Radke–Prausnitz model exponent [40,42].

Noticing the problem of the continuing increase in the adsorbed amount with an increase in concentration in the Freundlich equation, Sips [43] proposed an equation similar in form to the Freundlich equation; however, with a finite limit when the concentration is sufficiently high. At low adsorbate concentrations, it predicts a monolayer adsorption capacity with characteristics of the Langmuir isotherm, while at high concentrations it reduces to Freundlich isotherm [38].

$$q_e = \frac{Q_{\max} K_S C_e^{\,m_S}}{1 + K_S C_e^{\,m_S}} \tag{15}$$

where q_e is the adsorbed amount at equilibrium (mg g^{-1}), C_e is the equilibrium concentration of the adsorbate (mg L^{-1}), Q_{max} the Sips maximum adsorption capacity (mg g^{-1}), K_S is the Sips equilibrium constant (L mg^{-1}), and m_S is the Sips model exponent.

In order to evaluate the validity of isotherm equations, two different error functions of non-linear regression were employed to represent the experimental data, respectively. Linear determination coefficients (R^2) showed the fit between experimental data and linearized forms of isotherm equations while the average absolute deviation percentage (ΔQ) calculated according to Eq. (16) indicated the fit between the experimental and predicted values of adsorption capacity used for plotting isotherm curves. The applicability of the models was also verified through the residual root mean square error (RMSE), with the mathematical form given in Eq. (17) [44]:

$$\Delta Q(\%) = \frac{1}{N}\sum_{i=1}^{N}\left|\frac{q_{exp}-q_{calc}}{q_{exp}}\right|100 \quad (16)$$

$$RMSE = \sqrt{\frac{\sum_{i=1}^{N}(q_{exp}-q_{calc})^2}{N}} \quad (17)$$

where N is the number of experimental data and q_{exp} and q_{calc} stand for experimental and predicted (calculated) values. The smaller ΔQ and RMSE values indicate the better modeling.

2.2.3. Thermodynamic modeling

Thermodynamic considerations of an adsorption process are necessary to conclude whether the process is spontaneous or not. The Gibbs free energy change is an important criterion to determine the spontaneity of an adsorption system. Thermodynamic parameters such as the Gibbs free energy change ($\Delta G°$), enthalpy change ($\Delta H°$) and entropy change ($\Delta S°$) can be estimated using equilibrium constants changing with temperature [45]. $\Delta G°$ indicates the degree of spontaneity of the adsorption process and for significant adsorption to occur, $\Delta G°$ must be negative. The Gibbs free energy change of adsorption is defined as:

$$\Delta G° = -RT \ln K_{eq} \quad (18)$$

The K_{eq} value is calculated using the following equation:

$$K_{eq} = \frac{q_e}{C_e} \quad (19)$$

Relation between $\Delta G°$, $\Delta H°$ and $\Delta S°$ can be expressed by the following equations:

$$\Delta G° = \Delta H° - T\Delta S° \quad (20)$$

Eq. (20) can be written as:

$$\ln K_e = -\frac{\Delta G°}{RT} = -\frac{\Delta H°}{RT} + \frac{\Delta S°}{R} \quad (21)$$

According to the Eq. (21), $\Delta H°$ and $\Delta S°$ parameters can be calculated from the slope and intercept of the plot of ln K_{eq} vs. $1/T$, respectively [46].

3. Results and discussions

3.1. Characterization of ACs

The tendency of carbon to chemisorb oxygen is greater than the tendency to adsorb any other species. Oxygen chemisorbs on the surface of AC to form carbon–oxygen functional groups that may be acidic, neutral, or basic [20]. Results, presented in Table 2, show that the five ACs have very different chemical properties. The pH_{pzc} varies from 3.0 to 8.2, total acid functions vary from 0.20 to 1.57 meq g^{-1} and basic functions vary from 0.18 to 0.85 meq g^{-1}. There is one acidic AC (L27), three neutral (C1, F22 and S21), and one basic (X17). L27 and X17 are the ACs which presents the greatest number of surface groups.

The ACs also have different porous properties. The N_2 adsorption-desorption isotherms of the five ACs used show that L27, F22, and X17 are microporous but also contain some mesopores [47] as indicated by the shape and the hysteresis loop of the N_2 isotherms. Furthermore, the S21 is microporous only, which is confirmed by the values of its S_{micro} and S_{ext} (Table 3). The mean pore size (L_0) varied from 8.7 to 24.7 Å, the specific external surface (S_{ext}) varied from 43 to 444 $m^2 g^{-1}$ and the specific microporous volume (W_0) varied from 0.33 to 0.57 $cm^3 g^{-1}$.

3.2. Adsorption evaluation

3.2.1. Effect of adsorbent dosage

The effect of adsorbent dosage on the sorption process was investigated to obtain the optimum adsorbent amount to be used throughout the study. Fig. 1 shows the removal of 4-CP from 200 ppm aqueous solution by each of the five

Table 2
Chemical properties of activated carbons

	Acidic groups (meq. g^{-1})			Total acid groups (meq. g^{-1})	Total basic groups (meq. g^{-1})	Acidic/ Basic	pH_{pzc}	Character
	Carboxyl groups	Phenol groups	Lactone groups					
L27	0.81	0.30	0.46	1.57	0.18	8.72	3.0	Acidic
S21	0.05	0.30	0.03	0.38	0.33	1.06	7.4	Neutral
F22	0.13	0.14	0.05	0.32	0.26	1.23	7.5	Neutral
C1	0.24	0	0.03	0.27	0.23	0.96	7.2	Neutral
X17	0.15	0	0.02	0.17	0.85	0.24	8.2	Basic

Table 3
Textural properties of the granular activated carbons

Adsorbent material	W_o ($cm^3\ g^{-1}$)	L_o (Å)	S_{ext} ($m^2\ g^{-1}$)	S_{micro} ($m^2\ g^{-1}$)	S_{total} ($m^2\ g^{-1}$)	S_{BET} ($m^2\ g^{-1}$)
L27	0.57	18.5	444	616	1,060	1,575
S21	0.40	8.7	43	920	963	1,025
X17	0.33	14.3	157	462	619	956
F22	0.40	12.7	256	630	886	1,096
C1	0.44	24.7	162	356	518	787

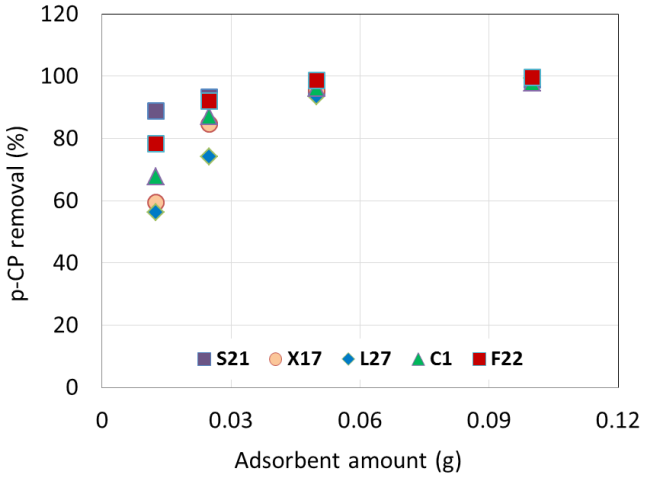

Fig. 1. Effect of adsorbent dose on 4-CP removal.

types of AC at different adsorbent doses (0.0125–0.1 g/50 mL), at 298 K.

According to Fig. 1, the removal of 4-CP increased with the adsorbent dose due to availability of greater amount of active sites on the surface of the adsorbent. It can also be seen that the uptake of solute increased up to the adsorbent dose of 0.05 g thereafter no significant increase was observed. Therefore, the adsorption degree at 0.05 g AC is very high; the percent removal varies between 95.43% and 98.90%. At sorbent amounts higher than 0.05 g the equilibrium concentration is close to zero. Therefore, the following experiments were conducted using an amount of 0.02 g adsorbent to differentiate among the sorption capacities of the AC.

3.2.2. *Effect of pH*

One of the most critical parameters in the treatment of chlorophenols by sorption that affects the surface potential of the adsorbent is the pH value of the coexisting liquid bulk phase [24]. The present study investigated the adsorption onto different ACs in various pH environments in order to determine the optimum pH conditions for 4-CP adsorption. The investigated pH conditions ranged between 2 and 12 at an initial 4-CP solution concentration of 200 mg L^{-1} as presented in Fig. 2. The obtained results showed that the relative removal of 4-CP remained constant for the L27 and increased slightly for the S21, F22, and X17 for initial pH of the solution from 2 to 8, followed by a significant decrease on sorption capacity at higher values of the pH. The maximum adsorption

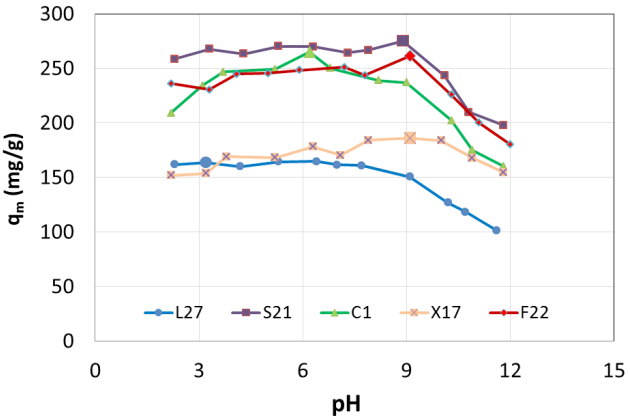

Fig. 2. Effect of initial pH on the adsorption of 4-CP.

capacity depends on the nature of the surface charge, such as for the acidic AC, L27, the maximum capacity was obtained until pH 7.7, whereas for the neutral AC, F22 and S21, the maximum capacities were reached at a pH value around 9. For the basic AC, X17, the highest capacity was obtained at the pH values from 8 to 10. Only the behavior of the neutral AC C1 was different, the sorption capacity increasing until pH 6 followed by a significant decrease with the pH values higher than 6.

Generally, the solution pH affects the surface charge of adsorbent and the degree of ionization of the adsorbate. At a solution pH lower than the pH_{pzc} the total surface charge will be on average positive, whereas at a higher value of solution pH it will be either neutral or negative. 4-CP as a weak acid compound with an acid dissociation constant (pKa) ≈ 9.37, is dissociated at pH > pKa, forming phenolate anions. Therefore, the adsorption decreases at high pH values due to both greater solubility of dissociated phenol (at pH > pKa) and less densely populated adsorption layers by increased repulsion forces between the dissociated form of the adsorbate and the carbon surface [48]. Furthermore, as pH increases the proportion of molecules in the undissociated (molecular) state will decrease, leading to a weaker activity. This explains the lower amount adsorbed at the basic values of pH compared with acid ones for the same equilibrium concentrations.

For the AC, C1 it is evident that the acidic and basic conditions diminish the adsorption capacity. At the pH 6.2, which is the unbuffered solution (close to neutral pH), the uptake of phenol is the highest (265 mg g^{-1}) and it decreases on either sides of this value. As Laszlo et al. [49] pointed out, when the adsorption takes place in unbuffered solutions (pH = 6.2), the carbon surfaces contain both protonated and deprotonated sites. The surface is more densely populated due to the combined acidic and basic interactions acting under these conditions. Increasing/decreasing the pH diminishes the strength of the interaction, and the adsorption performance.

3.3. *Adsorption kinetics*

The adsorption process was analyzed using three different kinetic models: the pseudo-first-order, pseudo-second-order and Weber–Morris intraparticle diffusion equations.

Table 4 lists the results of the rate constant studies for different initial 4-CP concentrations by the pseudo-first-order, second-order and intraparticle diffusion models.

Fig. 3 shows the kinetic data of adsorption at different initial solute concentrations plotted as adsorbed amounts vs. contact time, fitted with the pseudo-second-order model.

The comparison of the rate constants, k, calculated for different initial 4-CP concentrations by the pseudo-first-order and second-order models (Table 4) elucidated that rate constants decreased with the increase of the initial 4-CP concentration. The pseudo-second-order kinetic model described the adsorption kinetics with high correlation coefficients, greater than 0.96 for all the concentrations and adsorbents studied as also obtained elsewhere [26,50].

It is well-known that the pseudo-second-order kinetic model includes all the steps of adsorption including external film diffusion, adsorption, and internal particle diffusion, as also covered by Weber–Morris intraparticle diffusion model, which describes well the adsorption of 4-CP into porous media such as AC [50]. In the pseudo-second-order kinetic model, the time changes in dimensionless solid-phase concentration, $d(q_t/q_e)/d_t$, a form of adsorption rate, is proportional to the square of the residual amount of adsorption, $1 - (q_t/q_e)$. The k_2q_e value is a rate index and equals to the inverse of the half-life of adsorption process ($t_{0.5} = 1/k_2q_e$), which describes the kinetic performance affecting the fractional adsorption at any time [51].

The good linearized plots of t/q_t vs. t shown in Fig. 3 indicate the validity of the pseudo-second-order kinetic model. However, poor agreement with pseudo-first-order kinetic model was found due to bigger error margin of the resulted standard deviation.

To identify the diffusion mechanism of 4-CP adsorption onto AC, the intraparticle diffusion model, was used as shown in Fig. 4.

The plot of q_t against $t^{0.5}$ presents multi-linearity, which indicates that two or more steps occur. The first, sharper portion is attributed to the external surface adsorption or instantaneous adsorption stage. The second portion corresponds to the gradual adsorption stage, where the intraparticle diffusion is the rate-controlling step. In some cases, the third portion exists, which is the final equilibrium stage where the intraparticle diffusion starts to slow down due to extremely low solute concentrations in solution. If intraparticle diffusion occurs, then q_t vs. $t^{0.5}$ will be linear and if the plot passes through the origin, then the rate limiting process is only due

Table 4
Kinetic parameters for 4-CP adsorption onto activated carbon

AC	C_0 (mg/L)	q_{exp} (mg/g)	Pseudo-first-order			Pseudo-second-order			Intraparticle diffusion		
			q_{calc} (mg/g)	K_1 (h^{-1})	R^2	q_{calc} (mg/g)	K_2 (g/(mg h))	R^2	K_{dif} (mg/(g $h^{1/2}$))	I (mg/g)	R^2
C1	200	268.1	286.02	0.135	0.995	312.50	0.0004	0.975	61.215	–24.809	0.972
	160	224.08	189.67	0.119	0.887	256.41	0.001	0.943	62.642	–16.896	0.966
	120	212.43	181.26	0.055	0.878	243.90	0.0004	0.977	42.608	–17.629	0.942
	80	178.53	164.93	0.0624	0.925	212.77	0.0004	0.970	41.294	–23.732	0.971
	40	92.25	87.08	0.087	0.976	114.94	0.001	0.965	22.018	–12.254	0.838
L27	200	172.08	88.82	0.419	0.894	169.49	0.015	0.999	54.006	54.346	0.952
	160	157.18	84.94	0.573	0.592	158.73	0.017	0.999	51.467	54.12	0.967
	120	143.48	79.14	0.548	0.987	138.89	0.037	0.999	51.68	43.643	0.999
	80	119.93	51.11	0.285	0.794	120.48	0.013	0.999	43.794	35.844	0.999
	40	78.88	35.12	0.268	0.829	72.46	0.022	0.999	31.786	11.114	0.989
S21	200	282.6	183.15	0.164	0.872	294.12	0.002	0.998	73.873	42.813	0.794
	160	272.5	152.37	0.209	0.942	277.78	0.002	0.998	72.41	50.103	0.795
	120	259.33	152.83	0.0698	0.721	263.16	0.002	0.991	72.74	32.601	0.857
	80	192.23	90.34	0.112	0.937	200.00	0.003	0.999	66.054	12.303	0.951
	40	97.33	66.22	0.158	0.666	101.01	0.005	0.997	32.231	4.514	0.765
F22	200	267.28	202.35	0.241	0.864	270.27	0.002	0.999	81.481	27.636	0.921
	160	251.4	147.6	0.483	0.690	250.00	0.006	0.999	73.541	84.684	0.915
	120	226	100.16	0.151	0.755	227.27	0.004	0.999	63.099	61.247	0.916
	80	178.43	122.01	0.508	0.584	178.57	0.009	0.999	61.687	40.135	0.929
	40	97.3	72.93	0.607	0.654	95.24	0.029	0.999	39.13	16.983	0.868
X17	200	187.1	130.53	0.204	0.983	192.31	0.003	0.999	57.034	17.141	0.932
	160	180.55	128.5	0.156	0.932	188.68	0.003	0.999	59.75	2.277	0.958
	120	158.95	126.57	0.217	0.933	166.67	0.003	0.999	49.637	6.094	0.91
	80	143.2	95.15	0.086	0.883	149.25	0.002	0.998	38.347	4.949	0.942
	40	84.25	83.52	0.162	0.931	90.09	0.003	0.989	20.836	2.364	0.985

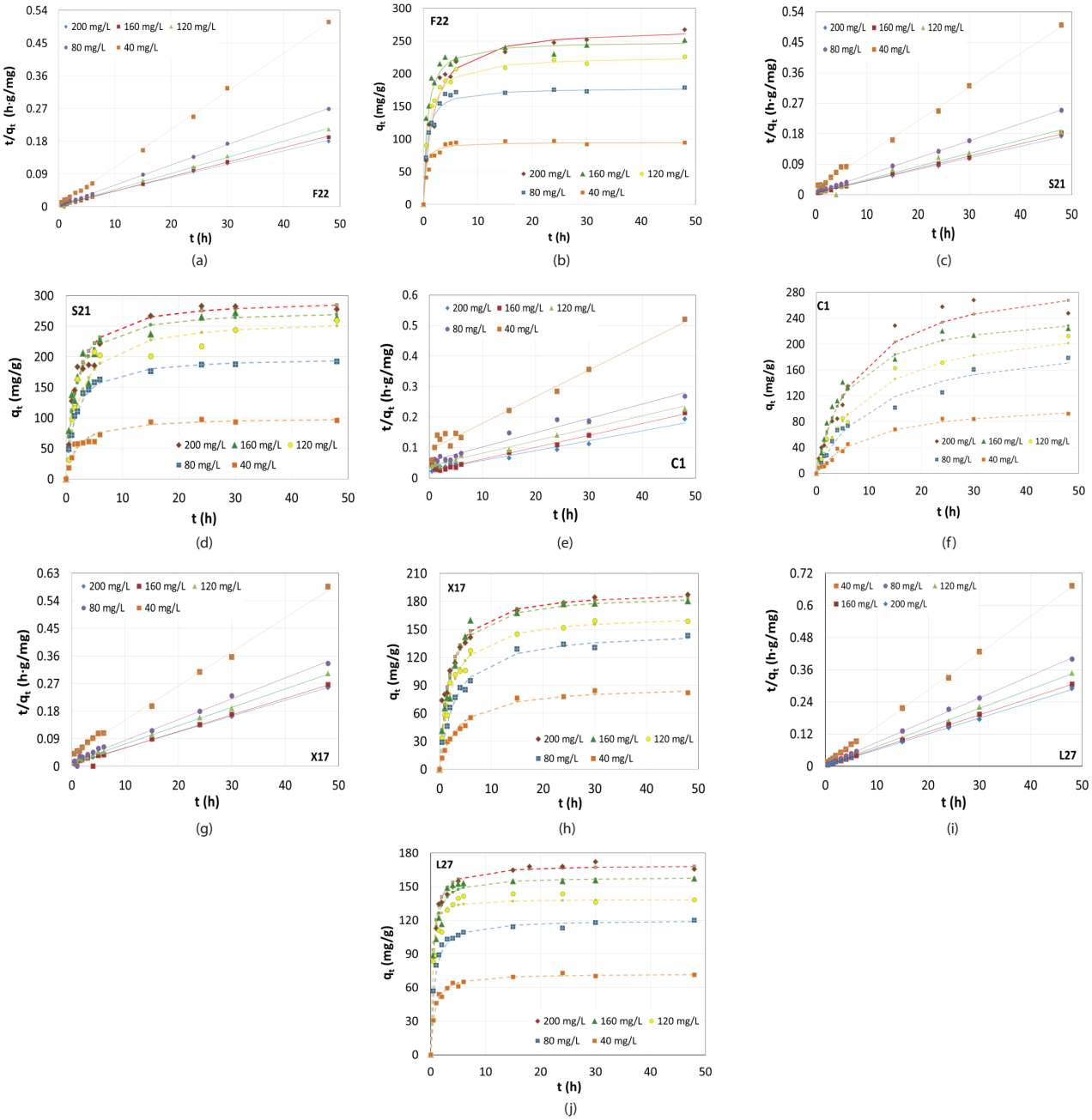

Fig. 3. (a) Pseudo-second-order kinetics for sorption of 4-CP at 298 K on F22 (a), S21 (c), C1 (e), X17 (g), L27 (i) and comparisons between experimental and predicted data for F22 (b), S21 (d), C1 (f), X17 (h), L27 (j).

to the intraparticle diffusion. Otherwise, some other mechanism along with intraparticle diffusion is also involved [52].

In this case, the slope of the first portion is not passing through the origin and it can be concluded that the film diffusion (boundary layer) controls the adsorption rate at the beginning of the adsorption process for all the materials. Referring to Fig. 4, the first stage was completed within the first 4 h for all initial concentrations, which depicts macro and mesopore diffusion [50] and the second stage of intraparticle diffusion control was then attained. This adsorption mechanism seems to explain the adsorption of 4-CP onto L27, when the sorbate is retained first in the mesopores, then in micropores until a final plateau is obtained. The third stage occurs only for L27 at lower initial concentrations. In case of the other sorbents (S21, F22, C1, and X17), the second linear step corresponds to the adsorption of 4-CP in micropores.

During the kinetic studies, the only changing parameters were time and concentration for all ACs (same temperature and shaking rate) which indicates that the external resistance to mass transfer surrounding the particles (*I*) of an adsorbent is not significantly changing. On the other hand the slope of the first portion becomes lower when the 4-CP

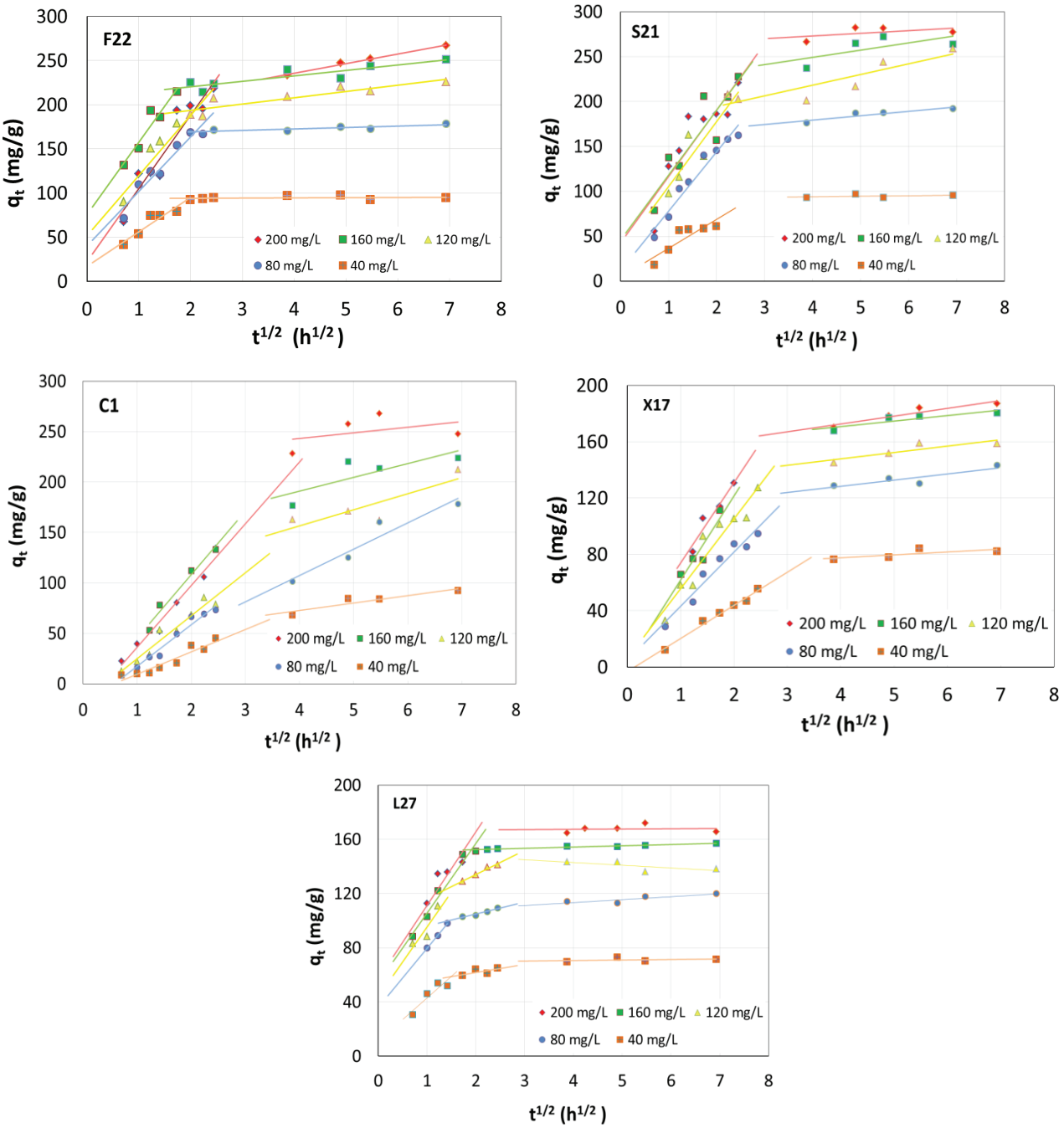

Fig. 4. Weber–Morris intra-particle diffusion plots for removal of 4-CP on AC.

initial solution concentration is also lower. Regarding X17, there are some deviations due to the different shape and sizes of the adsorbent particles. Besides, the C1 with the largest mean pore size (L_0 = 24.7 Å), among all the ACs, has negative I values for all the 4-CP initial concentrations investigated, which is to be expected and differs from the kinetic behavior of the other ACs.

The different portions of rates of adsorption indicated that the adsorption rate was initially faster and then slowed down when the time increased.

The constants were calculated and listed in Table 4.

3.4. Adsorption isotherms

The equilibrium data obtained at 298 K on the five different ACs were correlated by applying two and three parameter equilibrium models. Table 5 shows the values of isotherm parameters calculated by means of solver add-in function of the Microsoft Excel and those of the corresponding deviation percentage (ΔQ%) and root mean square error (RMSE). The values of deviations for the adsorption models are relatively low. Based on this criterium the three parameter models exhibited better fit to the sorption data than the

Table 5
Isotherm constants and their correlation coefficients for the adsorption of 4-CP onto ACs

Model	Parameters	Activated carbon														
		C1			L27			S21			F22			X17		
		25°C	35°C	45°C	25°C	35°C	45°C	25°C	35°C	45°C	25°C	35°C	45°C	25°C	35°C	45°C
Langmuir	K_L (L/mg)	0.08	0.07	0.17	0.05	0.05	0.04	0.41	0.41	0.76	0.47	0.41	0.31	0.09	0.06	0.05
	Q_{max} (mg/g)	250	236.39	210.67	190.22	161.29	153.85	276.72	260.92	135.6	244.39	243.22	231.09	199.53	197.85	198.27
	R_L (L/mg)	0.15	0.124	0.06	0.18	0.542	0.205	0.026	0.026	0.014	0.023	0.025	0.035	0.11	0.156	0.188
	RMSE	15.56	15.64	11.28	3.91	1.57	3.47	10.60	14.78	8.89	15.02	16.09	4.24	1.79	3.63	2.54
	Q (%)	7.72	10.45	6.56	3.26	0.98	2.32	5.78	7.80	12.33	8.22	7.87	6.59	1.30	1.36	1.77
Freundlich	K_F (L/mg)	46.56	42.91	73.77	34.24	33.49	25.76	117.32	110.43	96.97	111.00	101.00	88.96	57.26	42.16	36.82
	1/n	0.37	0.36	0.23	0.33	0.30	0.34	0.21	0.21	0.23	0.19	0.20	0.22	0.25	0.30	0.32
	RMSE	9.73	1.38	2.64	3.68	5.41	3.18	14.63	8.79	1.28	8.62	49.54	5.20	5.39	7.89	7.89
	Q (%)	5.42	0.68	1.66	3.00	4.92	2.50	8.19	4.86	0.51	5.20	5.34	2.42	3.88	6.14	1.25
Sips	Ks (L/mg)	0.09	0.14	0.27	0.07	0.05	0.05	0.30	0.49	0.48	0.39	0.38	0.33	0.11	0.06	0.05
	Q_{max} (mg/g)	304.02	280.16	234.8	204.97	163.02	162.26	281.45	274.09	272.18	336.03	330.78	316.32	209.8	198.14	197.36
	m_S	0.79	0.64	0.65	0.81	0.97	0.91	1.00	0.73	0.65	0.46	0.46	0.47	0.87	1.00	1.00
	RMSE	13.80	11.95	8.23	2.38	1.44	3.05	0.18	10.58	18.27	0.83	7.44	0.09	0.76	3.63	2.56
	Q (%)	4.94	6.18	3.35	1.41	1.16	2.78	3.11	4.87	9.06	0.30	3.32	0.76	0.38	2.47	1.90
Redlich–Peterson	$K_{R\text{-}Pe}$	21.16	31.35	52.43	14.93	8.03	9.14	83.91	147.91	167.39	281.85	238.76	97.79	18.50	11.61	9.07
	B (L/mg)	0.11	0.24	0.34	0.17	0.05	0.14	0.30	0.70	0.92	2.00	1.69	0.68	0.10	0.06	0.05
	β	0.93	0.89	0.94	0.85	0.99	0.83	1.00	0.95	0.93	0.87	0.87	0.89	0.99	0.99	1.00
	RMSE	14.99	13.58	9.35	1.34	1.45	1.92	6.33	12.07	19.75	1.16	8.57	2.05	1.61	3.62	2.57
	Q (%)	6.83	8.08	5.11	0.90	1.15	1.45	2.93	5.85	9.44	0.47	3.70	3.12	1.12	2.59	1.94
Radke–Prausnitz	$K_{R\text{-}P}$	0.11	0.13	0.34	0.06	0.05	0.04	0.37	1.61	133.36	0.84	0.85	0.62	0.10	0.06	0.05
	Q_{max} (mg/g)	194.03	173.13	153.13	162.50	158.76	144.35	247.55	152.27	97.46	193.65	175.33	171.12	186.93	192.64	197.93
	$m_{R\text{-}P}$	0.93	0.94	0.94	0.97	1.00	0.99	0.97	0.87	0.77	0.95	0.93	0.94	0.99	0.99	1.00
	RMSE	14.99	13.95	9.35	3.11	1.47	3.16	4.61	27.64	52.22	11.92	10.27	9.65	1.61	3.62	2.57
	Q (%)	6.82	9.31	5.10	2.61	1.21	2.94	4.39	5.85	13.58	5.93	5.09	4.52	1.12	2.59	1.94

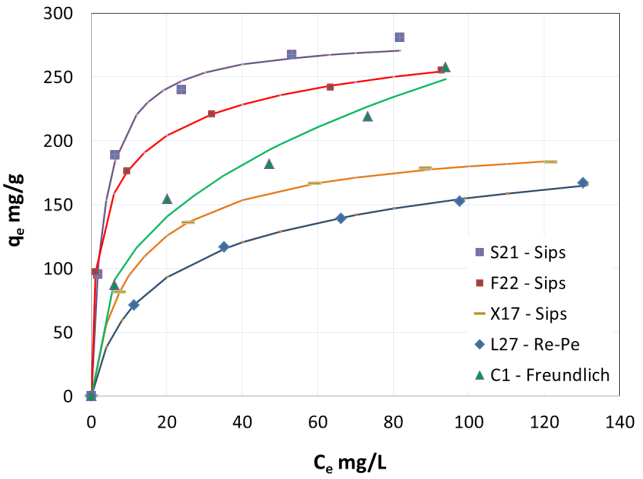

Fig. 5. Adsorption isotherms for AC S21, F22, and X17 modelled by Sips, L27 by Redlich–Peterson and C1 by Freundlich at 298 K.

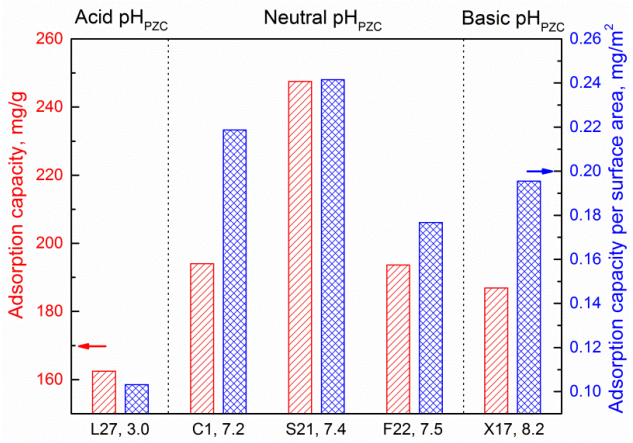

Fig. 6. Adsorption capacity and specific adsorption capacity dependence on the pH_{PZC} value.

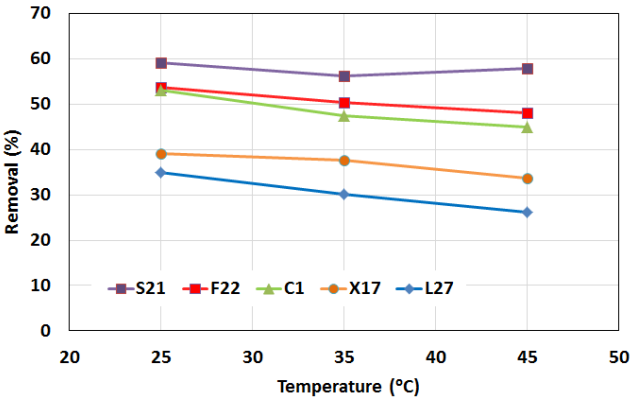

Fig. 7. Effect of temperature on 4-CP removal onto AC. (4-CP initial conc. 200 ppm).

two parameter models, Freundlich and Langmuir. The data fitted best with the Redlich–Peterson model for L27, Sips for F22, S21, and X17 and Freundlich for C1 which shows that the sorbents surfaces are not homogenous and contain more than one type of active sites [49]. Fig. 5 shows the experimental data and the predicted isotherms for the sorption of 4-CP onto all ACs at 298 K.

The largest sorption capacity was obtained in the order of S21>F22 >C1, all three having neutral surface characteristics. The mean pore size (L_0) varied in the increasing order from 8.7 to 24.7 Å, indicating that their sorbent textural characteristics directly affected the sorption capacity of AC (q_e). However when the acidic (L27) and basic (X17) ACs were considered, they exhibited lower sorption capacity, unproportional to their micropore area, compared with C1 (Table 3), emphasizing that the surface chemical properties determined the sorption capacity of the ACs.

In order to better understand the behavior of 4-CP adsorption onto ACs, the maximum values of adsorption capacity of the five ACs were compared as shown in Fig. 6. Also, the adsorption capacity per AC surface area was considered.

The value of pH_{pzc} of ACs seems to be of critical importance in the proper selection of sorbent. Therefore, in case of 4-CP neutral-surfaced ACs have the highest adsorption affinity. However, there are other factors that have to be taken into account. As pinpointed through the kinetic data, the adsorption rate of 4-CP on C1 is rather low most probably due to particle size.

3.5. Effect of temperature

To investigate the effect of temperature on adsorption capacity of the five ACs, several isotherm equilibrium experiments were conducted at 298, 308, and 318 K. Fig. 7 shows the effect of temperature on the removal of 4-CP at an initial concentration of 200 ppm.

The 4-CP removal was found to decrease with increasing temperature for all the investigated ACs showing that the adsorption process was exothermic in nature. The decrease in adsorption with the rise of temperature may be due to the weakening of adsorptive forces between the active sites of the adsorbent and adsorbate species and also between the vicinal molecules of the adsorbed phase [45,53]. This is also confirmed by the Q_{max} values of the two and three parameter fits for different values of temperature (Table 5).

Fig. 8 shows the influence of temperature on the sorption capacity of the five ACs, whereas the equilibrium data were fitted with each of the five considered models.

As can be noticed, the temperature influences the most the adsorption capacity of L27 that has the weakest adsorption properties towards 4-CP. On the other hand, in case of the sorbents with neutral surface characteristics, S21, F22, and C1, the temperature influences only marginally the adsorption capacity.

3.6. Adsorption thermodynamics

Values of the Gibbs free energy (ΔG°), enthalpy (ΔH°) and entropy (ΔS°) describing the thermodynamics of the investigated adsorption process were calculated based on

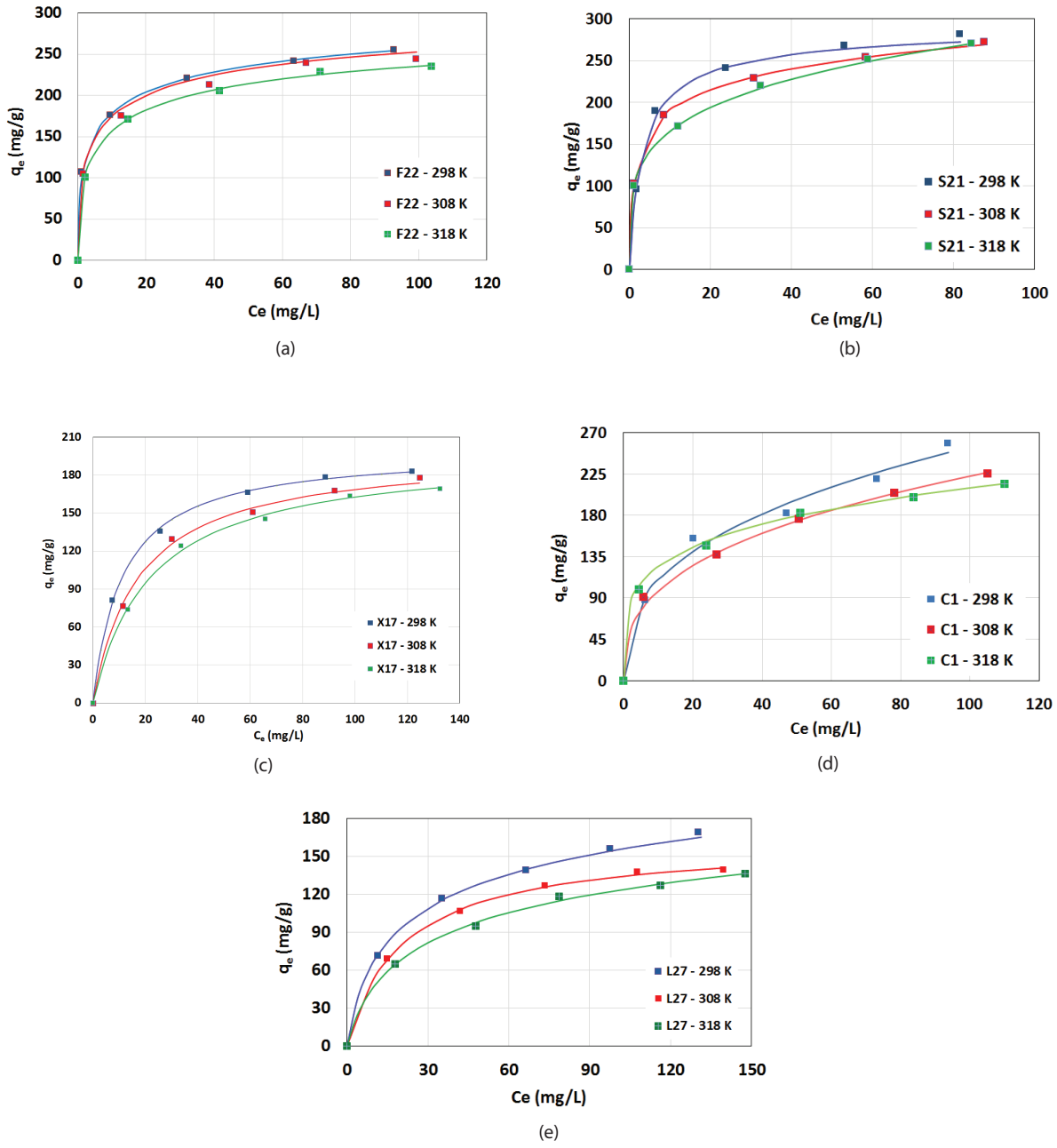

Fig. 8. Effect of temperature on sorption equilibrium on AC. Solid lines are calculated data according to Sips equation for F22 (a), Radke–Prausnitz for S21 (b), and X17 (c), Freundlich for C1 (d), and Redlich–Peterson for L27 (e).

the experimental runs carried out at different values of temperature (Table 6). The negative sign of $\Delta G°$ indicates that the process of the 4-CP adsorption onto AC is spontaneous in nature and thermodynamically feasible [45,54]. In this study, $\Delta G°$ values were found in the range of –1.6 to –8.3 kJ/mol, indicating that adsorption was physical in nature and spontaneous. ln$K$ values were positive. Negative values of $\Delta H°$ were determined for all the AC studied and their magnitude lay between –5.4 to –24.7 pointing to the exothermic process. $\Delta S°$ values obtained were positive for most of the ACs, which can be explained by the increased degrees of freedom of the 4-CP molecules in their adsorption state [31]. In fact, it shows the affinity of AC for 4-CP and the increasing randomness at the solid–solution interface during the adsorption process.

Besides, negative $\Delta G°$ values resulted from positive entropy contributions ($T\Delta S°$), suggested favorable adsorption due to an entropy-driven process [55].

4. Conclusions

The main goal of this investigation was to study the adsorption behavior of 4-CP onto AC in order to optimize the

Table 6
Thermodynamic parameters for the adsorption of 4-CP onto AC

AC	T (K)	K_{eq}	ΔG (kJ/mol)	ΔH (kJ/mol)	ΔS (J/mol K)
C1	298	6.25	–4.54	–6.89	7.89
	308	5.92	–4.56		
	318	7.47	–5.32		
L27	298	2.92	–2.65	–18.29	52.48
	308	2.22	–2.05		
	318	1.83	–1.60		
S21	298	20.31	–7.46	–5.39	–6.94
	308	24.39	–8.18		
	318	23.23	–8.32		
F22	298	26.30	–8.10	–24.72	55.76
	308	18.56	–7.48		
	318	14.05	–6.99		
X17	298	4.51	–3.73	–18.02	47.93
	308	3.37	–3.11		
	318	2.86	–2.78		

separation process based on the selection of sorbent having the proper textural and chemical characteristics. The kinetic study showed that 4-CP sorption on AC reaches equilibria fast. The rate determining step of the 4-CP adsorption was the microporous diffusion at low concentrations of sorbate. At high concentrations of 4-CP the adsorption process was controlled by the boundary layer between the 4-CP molecules in solution and AC active sorption sites. The value of pH_{pzc} of ACs proved to be a critical characteristic in the proper selection of sorbent. ACs with neutral surface properties showed the highest adsorption capacity for 4-CP, in the sequence of increasing order with increasing sorption micropore area. The AC C1 with neutral surface characteristics and the lowest micropore area exhibited higher sorption capacity than the acidic and basic ACs having higher micropore surface areas. This indicates that the effect of surface chemical characteristics on adsorption capacity is superior to the textural properties of AC. Under acidic conditions, 4-CP exists primarily in the toxic molecular (undissociated) form, while under basic conditions the dissociated form predominates leading to higher activity at low pH values. Sorption was exothermic, and thermodynamic parameters showed that the 4-CP adsorption onto AC was spontaneous in nature.

Acknowledgments

This work was supported by a grant of the Romanian National Authority for Scientific Research and Innovation, CNCS–UEFISCDI, project number PN-II-RU-TE-2014-4-0405.

We would like to especially thank CECA, Arkema Group France, for providing us with Aquasorb L27, X17, F22 and S21 granular activated carbon materials and to the Laboratories of Ege University, Department of Chemical Engineering, Izmir, Turkey, for assisting and supporting this work.

References

[1] M. Ahmaruzzaman, Adsorption of phenolic compounds on low-cost adsorbents: a review, Adv. Colloid Interface Sci., 143 (2008) 48–67.
[2] C. Namasivayam, D. Kavitha, Adsorptive removal of 2-chlorophenol by low-cost coir pith carbon, J. Hazard. Mater., 98 (2003) 257–274.
[3] L.F.G. Martins, M.C.B. Parreira, J.P. Prates Ramalho, P. Morgado, E.J.M. Filipe, Prediction of diffusion coefficients of chlorophenols in water by computer simulation, Fluid Phase Equilib., 396 (2015) 9–19.
[4] G. Mihoc, R. Ianos, C. Pacurariu, Adsorption of phenol and p-chlorophenol from aqueous solutions by magnetic nanopowder, Water Sci. Technol., 69 (2014) 385–391.
[5] K. Kusmierek, A. Swiatkowski, The influence of different agitation techniques on the adsorption kinetics of 4-chlorophenol on granular activated carbon, React. Kinet. Mech. Cat., 116 (2015) 261–271.
[6] S. Guilane, O. Hamdaoui, Desorption of 4-chlorophenol from spent granular activated carbon in continuous flow ultrasonic reactor, Desal. Wat. Treat., 57 (2016) 12708–12716.
[7] A. Gholizadeh, M. Kermani, M. Gholami, M. Farzadkia, Kinetic and isotherm studies of adsorption and biosorption processes in the removal of phenolic compounds from aqueous solutions: comparative study, J. Environ. Health Sci. Eng., 11 (2013) 1–10.
[8] Ihsanullah, H.A. Asmaly, T.A. Saleh, T. Laoui, V.K. Gupta, M.A. Atieh, Enhanced adsorption of phenols from liquids by aluminum oxide/carbon nanotubes: comprehensive study from synthesis to surface properties, J. Mol. Liq., 206 (2015) 176–182.
[9] F. Delval, G. Crini, J. Vebrel, Removal of organic pollutants from aqueous solutions by adsorbents prepared from an agroalimentary by-product, Bioresour. Technol., 97 (2006) 2173–2181.
[10] S. Al-Asheh, F. Banat, L. Abu-Aitah, Adsorption of phenol using different types of activated bentonites, Sep. Purif. Technol., 33 (2003) 1–10.
[11] M.D. Markovic, B.P. Dojcinovic, B.M. Obradovic, J. Nesic, M.M. Natic, T.B. Tosti, M.M. Kuraica, D.D. Manojlovic, Degradation and detoxification of the 4-chlorophenol by non-thermal plasma-influence of homogeneous catalysts, Sep. Purif. Technol., 154 (2015) 246–254.
[12] B. Deka, K.G. Bhattacharyya, Using coal fly ash as a support for Mn(II), Co(II) and Ni(II) and utilizing the materials as novel oxidation catalysts for 4-chlorophenol mineralization, J. Environ. Manage., 150 (2015) 479–488.
[13] Z. Li, D. Suzuki, C. Zhang, S. Yang, J. Nan, N. Yoshida, A. Wang, A. Katayama, Anaerobic 4-chlorophenol mineralization in an enriched culture under iron-reducing conditions, J. Biosci. Bioeng., 118 (2014) 529–532.
[14] Q.-S. Liu, T. Zheng, P. Wang, Y.-J. Li, Regeneration of 4-chlorophenol exhausted GAC with a microwave assisted wet peroxide oxidation process, Separ. Sci. Technol., 49 (2014) 68–73.
[15] Y.Y. Berestovskaya, V.V. Ignatov, L.N. Markina, A.A. Kamenev, O.E. Makarov, Degradation of ortho-chlorophenol, para-chlorophenol, and 2,4-dichlorophenoxyacetic acid by the bacterial community of anaerobic sludge, Microbiol., 69 (2000) 397–400.
[16] J.W. Birkett, J.N. Lester, Endocrine Disrupters in Wastewater and Sludge Treatment Processes, IWA Publishing, London, 2003.
[17] Z. Zhengguo, F. Xiaoqin, Y. Xiao-Xia, A. Fu-Qiang, Z. Wen-Xia, G. Jian-Feng, H. Tuo-Ping, W. Chin-Chuan, Effective adsorption of phenols using nitrogen-containing porous activated carbon prepared from sunflower plates, Korean J. Chem. Eng., 32 (2015) 1564–1569.
[18] L. De-Chang, D. Jin-Wen, Q. Ting-Ting, Z. Shun, J. Hong, Preparation of high adsorption performance and stable biochar granules by $FeCl_3$-catalyzed fast pyrolysis; RSC Advances, 6 (2016) 12226–12234.
[19] N.S. Kumar, M. Suguna, M.V. Subbaiah, A.S. Reddy, N.P. Kumar, A. Krishnaiah, Adsorption of phenolic compounds from aqueous solutions onto chitosan-coated perlite beads as biosorbent, Ind. Eng. Chem. Res., 49 (2010) 9238–9247.
[20] A. Dabrowski, P. Podkoscielny, Z. Hubicki, M. Barczak, Adsorption of phenolic compounds by activated carbon – a critical review, Chemosphere, 58 (2005) 1049–1070.

[21] M. Spiridon, O.R. Hauta, M.S. Secula, S. Petrescu, Preparation and characterization of some porous composite materials for water vapor adsorption, Rev. Chim. (Bucuresti), 63 (2012) 711–714.
[22] M.J. Ahmed, S.K. Theydan, Adsorption of *p*-chlorophenol onto microporous activated carbon from *Albizia lebbeck* seed pods by one-step microwave assisted activation, J. Anal. Appl. Pyrolysis, 100 (2013) 253–260.
[23] K.M. Park, H.G. Nam, K.B. Lee, S. Mun, Adsorption behaviors of sugars and sulfuric acid on activated porous carbon, J. Ind. Eng. Chem., 34 (2016) 21–26.
[24] K. Singh, B. Chandra, Adsorption behaviours of phenols onto high specific area activated carbon derived from *Trapa bispinosa*, Indian J. Chem. Technol., 22 (2015) 11–19.
[25] Z. Luo, M. Gao, S. Yang, Q. Yang, Adsorption of phenols on reduced-charge montmorillonites modified by bispyridinium dibromides: mechanism, kinetics and thermodynamics studies, Colloids Surf., A, 482 (2015) 222–230.
[26] L.-C. Zhou, X.-G. Meng, J.-W. Fu, Y.-C. Yang, P. Yang, C. Mi, Highly efficient adsorption of chlorophenols onto chemically modified chitosan, Appl. Surf. Sci., 292 (2014) 735–741.
[27] F. Stoeckli, Dubinins theory and its contribution to adsorption science, Russ. Chem. Bull., 12 (2001) 2265–2272.
[28] K.S.W. Sing, D.H. Everett, R.A.W. Paul, L. Moscou, R.A. Pierotti, J. Rouquerol, T. Domaniewska, Reporting physisorption data for gas/solid systems with special reference to the determination of surface area and porosity, Pure Appl. Chem., 57 (1985) 603–619.
[29] H.P. Boehm, E. Diehl, W. Heck, R. Sappok, Surface oxides of carbon, Angew. Chem., Int. Ed., 3 (1964) 669–677.
[30] J. Rivera-Utrilla, M. Sanchez-Polo, Ozonation of 1,3,6-naphthalenetrisulphonic acid catalysed by activated carbon in aqueous phase, Appl. Catal. B, 39 (2002) 319–329.
[31] Q.-S. Liu, T. Zheng, P. Wang, J.P. Jiang, N. Li, Adsorption isotherm, kinetic and mechanism studies of some substituted phenols on activated carbon fibers, Chem. Eng. J., 157 (2010) 348–356.
[32] B.H. Hameed, I.A.W. Tan, A.L. Ahmad, Adsorption isotherm, kinetic modeling and mechanism of 2,4,6-trichlorophenol on coconut husk-based activated carbon, Chem. Eng. J., 144 (2008) 235–244.
[33] S. Lagergren, B.K. Svenska, Zur theorie der sogenannten adsorption geloester stoffe, Vet.-A Handlingar, 24 (1898) 1–39.
[34] Y.S. Ho, G. McKay, A comparison of chemisorption kinetic models applied to pollutant removal on various sorbents, Proc. Saf. Environ. Protect., 76 (1998) 332–340.
[35] W.J. Weber, J.C. Morris, Kinetics of adsorption on carbon from solution, J. Sanity Eng. Div. Am. Soc. Civil Eng., 89 (1963) 31–59.
[36] I. Langmuir, The constitution and fundamental properties of solids and liquids, J. Am. Chem. Soc., 38 (1916) 2221–2295.
[37] H.M.F. Freundlich, Uber die adsorption in losungen, Z. Phys. Chem., 57 (1906) 385–470.
[38] O. Redlich, D.L. Peterson, A useful adsorption isotherm, J. Phys. Chem., 63 (1959) 1024–1026.
[39] O. Hamdaoui, E. Naffrechoux, Modeling of adsorption isotherms of phenol and chlorophenols onto granular activated carbon Part II. Models with more than two parameters, J. Hazard. Mater., 147 (2007) 401–411.
[40] C.J. Radke, J.M. Prausnitz, Adsorption of organic solutions from dilute aqueous solution on activated carbon, Ind. Eng. Chem. Fundam., 11 (1972) 445–451.
[41] D. Schimmel, K.C. Fagnani, J.B. Oliveira dos Santos, M.A.S.D. Barros, E. Antonio da Silva, Adsorption of turquoise blue QG reactive bye commercial activated carbon in batch reactor: kinetic and equilibrium studies, Braz. J. Chem. Eng., 27 (2010) 289–298.
[42] R. Ocampo-Pérez, M.M. Abdel Daiem, J. Rivera-Utrilla, J.D. Méndez-Díaz, M. Sánchez-Polo, Modeling adsorption rate of organic micropollutants present in landfill leachates onto granular activated carbon, J. Colloid Interface Sci., 385 (2012) 174–182.
[43] R. Sips, On the structure of a catalyst surface, J. Phys. Chem., 16 (1948) 490–495.
[44] M.S. Secula, I. Cretescu, M. Diaconu, Adsorption of acid dye Eriochrome Black T from aqueous solutions onto activated carbon. Kinetic and equilibrium studies, J. Environ. Prot. Ecol., 15 (2014) 1583–1593.
[45] M. Kilic, E. Apaydin-Varol, A.E. Putun, Adsorptive removal of phenol from aqueous solutions on activated carbon prepared from tobacco residues: equilibrium, kinetics and thermodynamics, J. Hazard. Mater., 189 (2011) 397–403.
[46] K.V. Kumar, K. Porkodi, Relation between some two- and three-parameter isotherm models for the sorption of methylene blue onto lemon peel, J. Hazard. Mater., 138 (2006) 633–635.
[47] M.S. Secula, B. Cagnon, T. Ferreira de Oliveira, O. Chedeville, H. Fauduet, Removal of acid dye from aqueous solutions by electrocoagulation/GAC adsorption coupling: kinetics and electrical operating costs, J. Taiwan. Inst. Chem. Eng., 43 (2012) 767–775.
[48] D.A. Blanco-Martínez, L. Giraldo, J.C. Moreno-Piraján, Effect of the pH in the adsorption and in the immersion enthalpy of monohydroxylated phenols from aqueous solutions on activated carbons, J. Hazard. Mater., 169 (2009) 291–296.
[49] K. Laszlo, P. Podkoscielny, A. Dabrowski, Heterogeneity of activated carbons with different surface chemistry in adsorption of phenol from aqueous solutions, Appl. Surf. Sci., 252 (2006) 5752–5762.
[50] C. Valderrama, X. Gamisans, X. de las Heras, A. Farran, J.L. Cortina, Sorption kinetics of polycyclic aromatic hydrocarbons removal using granular activated carbon: intraparticle diffusion coefficients, J. Hazard. Mater., 157 (2008) 386–396.
[51] F.-C. Wu, R.-L. Tseng, S.-C. Huang, R.-S. Juang, Characteristics of pseudo-second-order kinetic model for liquid-phase adsorption: a mini-review, Chem. Eng. J., 151 (2009) 1–9.
[52] H.B. Senturk, D. Ozdes, A. Gundogdu, C. Duran, M. Soylak, Removal of phenol from aqueous solutions by adsorption onto organomodified Tirebolu bentonite: equilibrium, kinetic and thermodynamic study, J. Hazard. Mater., 172 (2009) 353–362.
[53] J.R. Kim, S.G. Huling, E. Kan, Effects of temperature on adsorption and oxidative degradation of bisphenol A in an acid-treated iron-amended granular activated carbon, Chem. Eng. J., 262 (2015) 1260–1267.
[54] L. Zhang, B. Zhang, T. Wu, D. Sun, Y. Li, Adsorption behavior and mechanism of chlorophenols onto organoclays in aqueous solution, Colloids Surf. A, 484 (2015) 118–129.
[55] P. Li, A.K. SenGupta, Entropy-driven selective ion exchange for aromatic ions and the role of cosolvents, Colloids Surf. A: Physicochem. Eng. Asp., 191 (2001) 123–132.